COMMUNICATIONS PHYSICS

ARTICLE

https://doi.org/10.1038/s42005-019-0192-y OPEN

Concurrent atomic force spectroscopy

Carolina Pimenta-Lopes [1,2,3], Carmen Suay-Corredera [1,3], Diana Velázquez-Carreras [1], David Sánchez-Ortiz[1] & Jorge Alegre-Cebollada [1]

Force-spectroscopy by atomic force microscopy (AFM) is the technique of choice to measure mechanical properties of molecules, cells, tissues and materials at the nano and micro scales. However, unavoidable calibration errors of AFM probes make it cumbersome to quantify modulation of mechanics. Here, we show that concurrent AFM force measurements enable relative mechanical characterization with an accuracy that is independent of calibration uncertainty, even when averaging data from multiple, independent experiments. Compared to traditional AFM, we estimate that concurrent strategies can measure differences in protein mechanical unfolding forces with a 6-fold improvement in accuracy or a 30-fold increase in throughput. Prompted by our results, we demonstrate widely applicable orthogonal fingerprinting strategies for concurrent single-molecule nanomechanical profiling of proteins.

[1] Centro Nacional de Investigaciones Cardiovasculares Carlos III (CNIC), 28029 Madrid, Spain. [2] Present address: Department of Physiological Sciences, University of Barcelona, Barcelona, Spain. [3] These authors contributed equally: Carolina Pimenta-Lopes, Carmen Suay-Corredera. Correspondence and requests for materials should be addressed to J.A.-C. (email: jalegre@cnic.es)

The development of atomic force microscopy (AFM) has enabled imaging the nanoscale with unprecedented length resolution, revolutionizing nanotechnology, materials science, chemistry, and biology[1–3]. AFM is based on the detection of interaction forces between a sample and a microfabricated cantilever, the force probe of the technique. Traditionally, low-scanning speeds have limited the reach of AFM; however, recent developments involving miniaturized cantilevers have achieved imaging at video frame rates, launching the field of high-speed AFM[4]. The ability of AFM to measure forces at the nano and micro scale can be exploited to quantify mechanical parameters such as stiffness, viscoelasticity, or adhesion forces, while simultaneously imaging surface topology[2,5,6]. Due to its force sensitivity down to picoNewtons (pN), AFM-based force spectroscopy, or simply atomic force spectroscopy, can also be used to examine single-molecule dynamics and ligand–receptor interactions under force[7–9] of relevance for cellular stiffness, mechanosensing, and mechanotransduction[10–13].

A key limitation of atomic force spectroscopy stems from uncertain calibration of the spring constant (k_{sc}) of the AFM cantilever, which is needed to determine force values[14]. Different calibration methods to estimate k_{sc} have been developed, differing in their simplicity, damage to the cantilever tip, experimental compatibility, and associated uncertainty. Estimates of calibration uncertainty (CU) up to 25% are usually reported;[15] however, even higher inaccuracies can result from defects in individual cantilevers, and from unpredictable changes in k_{sc} during experimentation due to material deposition, mechanical drift, and wear[7,16].

Force calibration uncertainties in AFM lead to inaccurate quantification of mechanical properties, a situation that is worsened in modes where the elusive geometry of the cantilever tip is required to extract mechanical information[17]. Indeed, relative AFM studies to characterize mechanical modulation of proteins, materials, and cells are challenging, since they necessitate multiple experiments, each one affected by different calibration errors (Fig. 1a)[18,19]. As a result, there is a pressing need to develop methods that can overcome inaccurate AFM force calibration[18]. Averaging results from several experiments obtained with different cantilevers can reduce the systematic error, since individual calibration errors are more probable to be averaged out as more experiments are included in the analysis[20]. The drawback of this method, which we refer to as traditional atomic force spectroscopy, is a considerable loss of throughput of the technique.

In theory, a manner to overcome calibration errors in relative atomic force spectroscopy is to measure the samples in a single experiment using one cantilever under the same calibration parameters, which we term concurrent atomic force spectroscopy (Fig. 1b)[21]. Indeed, concurrent mechanical characterization of several proteins in a single experiment has been achieved using microfluidics, on-chip protein patterning, and force spectroscopy measurements in custom-built atomic force/total internal reflection fluorescence microscopes[22,23]. However, this advanced technology is not available to most AFM users, and the extent of improvement in performance by concurrent AFM remains unexplored.

Here, we use error propagation analysis and Monte Carlo simulations to examine how force calibration errors impact determination of mechanical properties of proteins by atomic force spectroscopy, and demonstrate the remarkable improvement that stems from concurrent measurements. We find that averaging results from multiple concurrent experiments retains statistical power, leading to drastically improved accuracy and throughput in the determination of relative mechanical properties by AFM. Prompted by our findings, we have developed orthogonal fingerprinting (OFP) as a simple and widely applicable strategy for concurrent single-molecule nanomechanical profiling of proteins (Fig. 1c).

Results

Interexperimental errors in traditional force spectroscopy. To understand how errors in calibration of AFM lead to inaccurate determination of mechanical properties, we have measured protein mechanical stability by single-molecule force spectroscopy AFM[7] (Fig. 2a, Supplementary Fig. 1). This AFM mode is very well suited to examine propagation of calibration errors since protein unfolding forces are obtained directly from experimental data and do not depend on further modelling or approximations.

We first measured the resistance to mechanical unfolding of the same protein in different, independently calibrated atomic force spectroscopy experiments. We produced a polyprotein containing eight repetitions of the C3 domain of human cardiac myosin-binding protein C (Supplementary Fig. 2, Supplementary Note 1) and subjected individual $(C3)_8$ polyproteins to a linear increase in force of 40 pN s^{-1} using a force-clamp AFM. Results from two independent experiments are shown in Fig. 2b, c. In any given AFM experiment, several single-molecule events coming from different molecules are recorded with a single cantilever, under the same calibration parameters. In these single-molecule

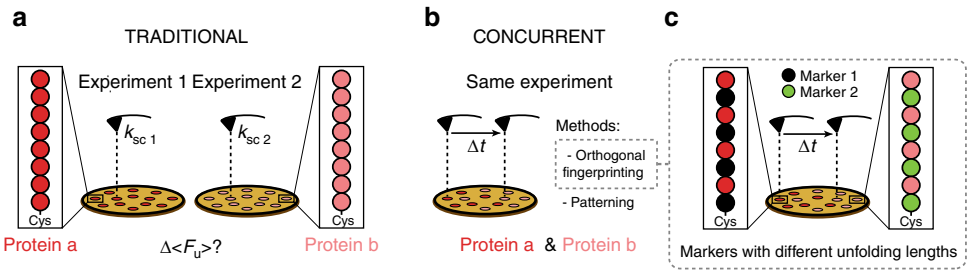

Fig. 1 Atomic force spectroscopy approaches to compare unfolding forces of two proteins. **a** Traditional strategy. The difference in mean unfolding force, $\Delta\langle F_u\rangle$, of Protein a and Protein b is estimated from different atomic force microscopy (AFM) experiments done under different calibration parameters (k_{sc1} and k_{sc2}). C-terminal cysteine residues used for covalent tethering to gold-covered coverslips are shown. **b** Concurrent strategy. By sampling Protein a and Protein b in the same experiment, calibration errors affect determination of the unfolding forces of both proteins equally. Hence, the accuracy in determination of $\Delta\langle F_u\rangle$ is improved. In concurrent strategies, either Protein a or Protein b are probed in different pulling attempts happening at different times within the same AFM experiment (temporal sequence is represented by Δt). Concurrent atomic force spectroscopy can be achieved using protein patterning methods[22] or by orthogonal fingerprinting, as described in this report. **c** Orthogonal fingerprinting is based on concurrent AFM measurements of heteropolyproteins that include marker domains with different fingerprinting unfolding lengths. Both heteropolyproteins are homogeneously distributed on the surface and are picked up randomly throughout the same AFM experiment

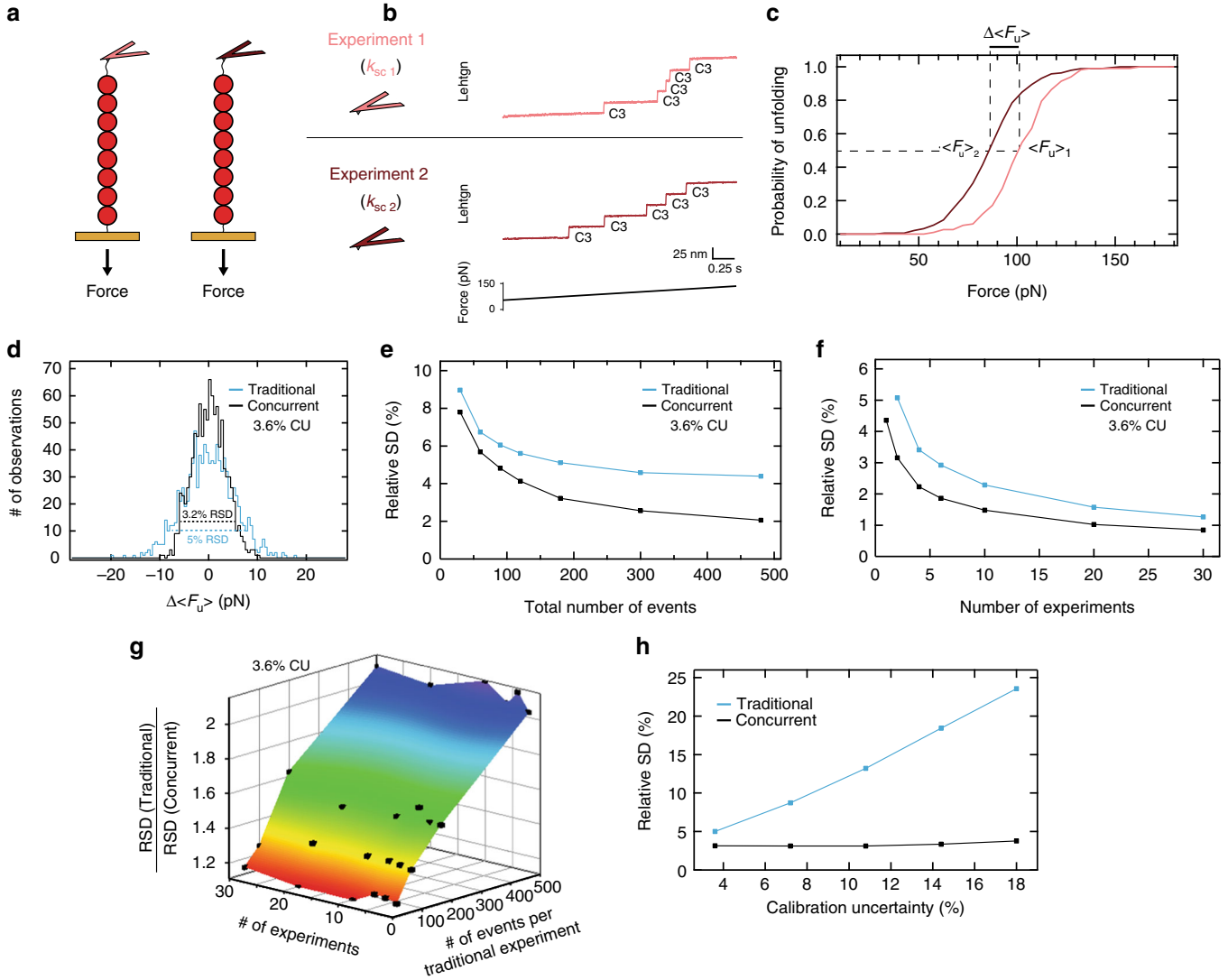

Fig. 2 Concurrent mechanical profiling by atomic force spectroscopy. **a** Schematic representation of traditional single-molecule atomic force spectroscopy, in which data are obtained in multiple, independent experiments under different force calibration parameters. **b** Results from two independent atomic force microscopy (AFM) experiments in which a $(C3)_8$ polyprotein is pulled. Due to uncertain calibration of the cantilever's spring constant (k_{sc}), force values are affected by errors that differ between experiments. We show two individual unfolding traces of the $(C3)_8$ polyprotein, in which mechanical unfolding events of individual C3 domains are detected by increases of 24 nm in the length of the polyprotein. **c** Experimental cumulative unfolding probability distributions obtained from 117 (Experiment 1) and 191 (Experiment 2) C3 unfolding events. The corresponding $\langle F_u \rangle$ values are 98.7 and 82.9 pN, respectively. **d** Distributions of $\Delta\langle F_u \rangle$ obtained by Monte Carlo simulations, considering the same total number of experiments and unfolding events for both traditional (blue) and concurrent measurements (black). We considered two experiments, 200 total unfolding events per protein, and a 3.6% force calibration uncertainty (CU). **e** Relative standard deviation (RSD) of the distribution of $\Delta\langle F_u \rangle$ decreases with the total number of unfolding events both in traditional (blue) and in concurrent measurements (black). Number of experiments is 2. **f** Keeping the same number of events per experiment ($n_{\text{events per experiment}} = 200$, in the traditional approach, and 100 in the concurrent strategy), the RSD of the distribution of $\Delta\langle F_u \rangle$ decreases with the number of experiments (blue: traditional; black: concurrent). **g** The relative improvement in the RSD of $\Delta\langle F_u \rangle$ distributions by the concurrent strategy increases with the number of events per experiment, and remains fairly insensitive to the number of averaged experiments. **h** RSD of the distributions of $\Delta\langle F_u \rangle$ at increasing CU for the traditional (blue) and the concurrent (black) strategies. The remaining simulation parameters are as in **d**. In **d**–**h**, the number of events per experiment and protein in the concurrent approach was half of the number of events in the traditional strategy so that RSDs are compared between conditions with equal total number of events

recordings, the stochastic unfolding of individual C3 domains by mechanical force can be detected as 24 nm step increases in the length of the polyprotein (Fig. 2b; Supplementary Fig. 3A). We measured the force at which the unfolding events occur and calculated distributions of unfolding forces[24]. Despite the fact that both distributions are well defined ($n > 115$ unfolding events), the difference in their mean unfolding force ($\Delta\langle F_u \rangle$) is 19% (Fig. 2c). The magnitude of this interexperimental variation is in agreement with the spread of $\langle F_u \rangle$ values reported in the literature for other proteins[20]. These differences can mask comparable changes in mechanical properties induced by disease-causing mutations[19] or post-translational modifications[25], which is a key limitation of traditional single-molecule atomic force spectroscopy.

Interexperimental variations in $\langle F_u \rangle$ of proteins are typically interpreted in terms of different errors in the calibration of AFM cantilevers, a procedure that can entail 25% uncertainty[7,14,15,22]. We used Monte Carlo simulations to examine how errors originating from uncertain cantilever calibration propagate to

$\langle F_u \rangle$ values measured by atomic force spectroscopy experiments (see Methods). Briefly, in each simulated experiment we impose an error to the force that is randomly drawn from a normal distribution defined by a relative standard deviation (RSD) that is equal to the considered calibration uncertainty. After definition of the error in force for a cycle, a kinetic Monte Carlo algorithm is used to obtain distributions of unfolding forces for a given number of protein domains subjected to a nominal 40 pN s^{-1} increase in force. For each one of the 1000 cycles of the simulation, we calculate the corresponding $\Delta\langle F_u \rangle$ considering a certain number of independent experiments, each one affected by a different calibration error. Simulations return the distribution of $\Delta\langle F_u \rangle$ values obtained in the 1000 cycles. The spread of the distribution, which is a measure of the accuracy of atomic force spectroscopy data, is quantified by its RSD.

Using our Monte Carlo procedure, we have simulated mechanical protein unfolding under a modest 3.6% force calibration uncertainty. This value is a good estimate of the lowest uncertainty that can be achieved by the thermal fluctuations method, typically used in single-molecule AFM studies (Supplementary Note 2, Supplementary Fig. 4)[7]. Figure 2d shows the simulated distribution of $\Delta\langle F_u \rangle$ obtained from two independent experiments in which the same protein is probed (200 unfolding events per experiment). It is remarkable that two mean unfolding forces obtained in different cycles can differ by more than 25% (Supplementary Fig. 5A). Hence, although conservative, a mere 3.6% inaccuracy in cantilever calibration can explain considerably higher differences in $\langle F_u \rangle$ obtained in traditional atomic force spectroscopy experiments.

Accuracy in $\Delta\langle F_u \rangle$ by concurrent atomic force spectroscopy. We have used our Monte Carlo simulations to estimate the accuracy in $\Delta\langle F_u \rangle$ achieved by concurrent measurement of the mechanical stability of two proteins. Considering equal total number of events and experiments, and a 3.6% calibration uncertainty, we find that the RSD of the distribution of $\Delta\langle F_u \rangle$ decreases from 5.0 to 3.2% when measurements are taken concurrently (Fig. 2d). RSD values are further reduced at higher number of unfolding events, as expected from better definition of the distribution of unfolding forces (Fig. 2e, Supplementary Fig. 5B). Interestingly, averaging multiple concurrent experiments leads to reductions in RSD, despite the fact that each individual experiment is performed under different calibration parameters (Fig. 2f). Increasing the number of events or experiments also results in lower RSD values when proteins are probed in traditional, separate experiments (Fig. 2e, f). We find that the relative improvement in RSD achieved by concurrent over traditional atomic force spectroscopy increases with the number of unfolding events per experiment, and remains fairly constant at increasing number of experiments (Fig. 2g). Hence, we conclude that averaging independent atomic force spectroscopy experiments, in which two proteins are probed concurrently, retains the statistical power, even if those individual experiments are affected by different calibration errors.

All our simulations in Fig. 2d–g were run considering 3.6% uncertainty in force calibration, which is much smaller than usually reported[7,14,15,22]. Hence, we estimated the RSD of the distribution of $\Delta\langle F_u \rangle$ at increasing calibration uncertainties. As expected, higher calibration uncertainties lead to much increased RSD in traditional atomic force spectroscopy, whereas the RSD of concurrent distributions remains insensitive to calibration uncertainty (Fig. 2h), even when data from several independent experiments are averaged (Supplementary Fig. 6A).

OFP for concurrent force spectroscopy. Our simulation results show that under a modest 3.6% uncertainty in force, concurrent atomic force spectroscopy measurements can reach the same level of accuracy in $\Delta\langle F_u \rangle$ with 2–4 times less experiments than the traditional approach (Fig. 2f). Furthermore, at high values of calibration uncertainty, the accuracy in $\Delta\langle F_u \rangle$ of concurrent measurements can be 6 times higher than in the traditional approach (Fig. 2h). These improvements in throughput and accuracy prompted us to design a general strategy for concurrent measurements of mechanical properties of proteins that can be readily applied to any AFM-based force spectrometer.

Having methods to identify single-molecule events is a fundamental requirement of force spectroscopy AFM. In the case of mechanical characterization of proteins, this need is fulfilled by the use of polyproteins, which provide molecular fingerprints that easily discriminate single-molecule events from spurious, non-specific interactions[26,27] (Supplementary Fig. 3). As exemplified in Fig. 2b, mechanical unfolding of polyproteins produces repetitive events whose length fingerprints the domain of interest. If two polyproteins are to be measured concurrently in the same experiment, it is imperative that they have different fingerprinting unfolding lengths. Here, we propose a widely applicable manner of achieving such OFP through the use of heteropolyproteins, in which marker proteins are fused to the proteins of interest[28] (Fig. 1c). Since OFP identifies proteins through the unfolding length of the marker domains, proteins of interest to be compared can have the same unfolding length (e.g., mutant or biochemically modified proteins). To test whether heteropolyproteins can be employed to achieve OFP during concurrent measurement of proteins by atomic force spectroscopy, we have measured the mechanical stability of the C3 domain in different polyprotein contexts (Fig. 3a, 4a).

We first followed a single-marker strategy using the heteropolyprotein $(C3\text{-}L)_4$ (Fig. 3, Supplementary Fig. 2, and Supplementary Note 1). In $(C3\text{-}L)_4$, we used Protein L as a marker since its unfolding length is different from the one of C3[20]. Indeed, mechanical unfolding of $(C3\text{-}L)_4$ under a 40 pN s^{-1} ramp results in the appearance of 16 and 24 nm steps, which correspond, respectively, to the unfolding of L and C3 domains (Fig. 3b, Supplementary Fig. 3B). We selected unfolding traces of $(C3)_8$ and $(C3\text{-}L)_4$, obtained in independent, traditional experiments, and classified them according to the number of 16 and 24 nm events they contain. Our results show that a gating criterion of $n(16\,\text{nm}) = 0$ and $n(24\,\text{nm}) > 2$ unambiguously identifies traces coming from $(C3)_8$, whereas traces resulting from $(C3\text{-}L)_4$ can be safely assigned when $n(16\,\text{nm}) > 1$ and $0 < n(24\,\text{nm}) < 5$ (Fig. 3b). We analyzed 17 such traditional experiments and obtained distributions of unfolding forces for C3 in the context of both polyproteins, which we found to be very similar ($\langle F_u \rangle = 90.7$ and 88.4 pN for the homo- and the heteropolyproteins, respectively, Fig. 3c, Table 1). We used our Monte Carlo simulations to estimate the RSD associated to $\Delta\langle F_u \rangle$ that is expected from the actual number of experiments and events obtained (Fig. 3c, Table 1, Supplementary Fig. 7A).

Following validation of the polyprotein gating criterion (Fig. 3b), we measured $(C3)_8$ and $(C3\text{-}L)_4$ concurrently in OFP experiments. Single-molecule traces were classified according to the number of 16 and 24 nm steps they contain, and sorted as coming from $(C3)_8$ or $(C3\text{-}L)_4$ before analysis of unfolding data (Fig. 3d). As in the case of traditional experiments, the unfolding probability distributions of C3 in the context of $(C3)_8$ and $(C3\text{-}L)_4$ are very similar ($\langle F_u \rangle = 96.3$ and 93.4 pN for the homo- and the heteropolyproteins, respectively, Fig. 3e, Table 1). However, only five OFP experiments were required to reach a lower RSD than in traditional AFM, a 3 times higher speed of data acquisition (Fig. 3c, e, Table 1, Supplementary Fig. 7A).

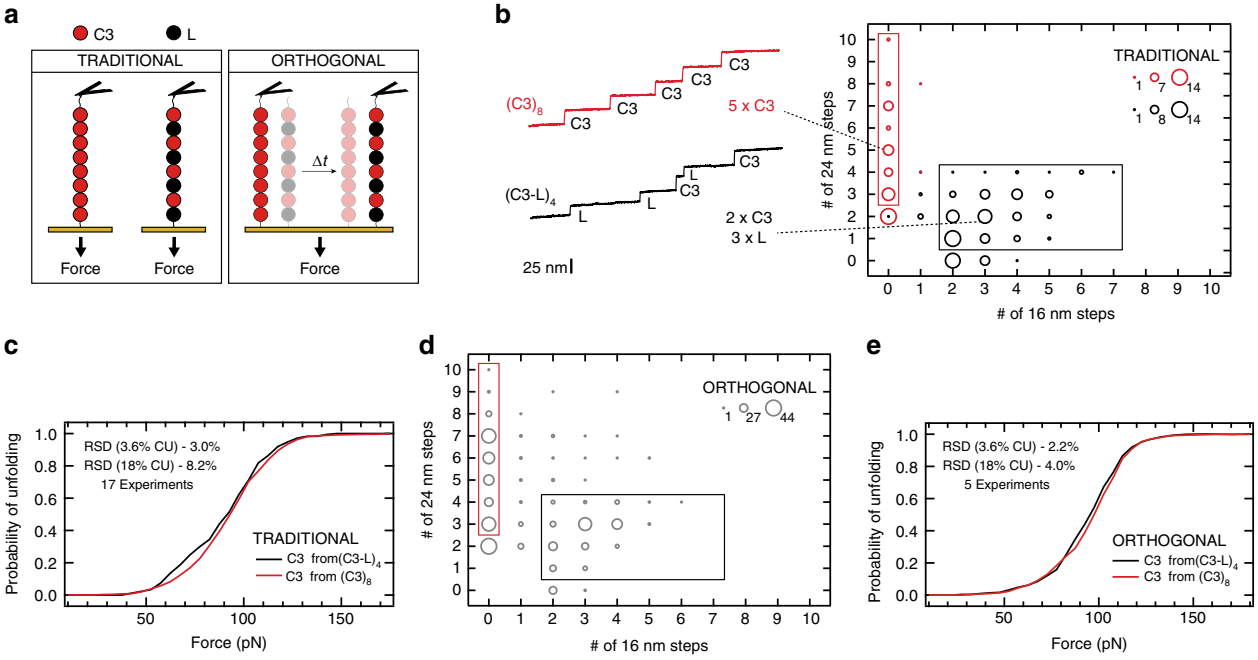

Fig. 3 Orthogonal fingerprinting (OFP) enables concurrent measurement of proteins. **a** In traditional experiments, $(C3)_8$ and $(C3\text{-}L)_4$ are measured in different atomic force microscopy (AFM) experiments, while in OFP, either one or the other protein are measured in single pulling attempts within the same AFM experiment (temporal sequence is represented by Δt; the protein being pulled at each time is highlighted). **b** Mechanical unfolding of $(C3)_8$ (red) and $(C3\text{-}L)_4$ (black) were measured in separate experiments. Individual traces were classified according to the number of 16 and 24 nm steps they contain. We show representative unfolding traces of one $(C3)_8$ molecule (red), in which five 24 nm unfolding events are detected, and one $(C3\text{-}L)_4$ polyprotein (black), comprising two 24 nm and three 16 nm unfolding events. The graph plot shows the frequency of the traces that have different combinations of unfolding events, as indicated by the size of the dots. The rectangles represent gating strategies that identify traces coming from $(C3)_8$ or $(C3\text{-}L)_4$. Number of traces: $(C3)_8$, 59; $(C3\text{-}L)_4$, 129. **c** Experimental cumulative unfolding probability distribution of the C3 domain in the context of $(C3)_8$ (11 experiments, 1334 events, red) and $(C3\text{-}L)_4$ (6 experiments, 177 events, black), following traditional AFM. **d** $(C3)_8$ and $(C3\text{-}L)_4$ polyproteins were measured concurrently by orthogonal fingerprinting (OFP). 468 traces were classified according to the number of 16 and 24 nm events. The plot shows the frequency of the traces that have different combinations of unfolding events, as indicated by the size of the dots. The gating criterion defined in **b** allows the classification of individual traces as resulting from $(C3)_8$ (red rectangle) or $(C3\text{-}L)_4$ (black rectangle). **e** Experimental cumulative unfolding probability distribution of the C3 domain in the context of $(C3)_8$ (625 events, red) and $(C3\text{-}L)_4$ (311 events, black), resulting from unfolding data obtained in five independent OFP experiments. Relative standard deviation (RSD) values in the insets in **c**, **e** are estimated using Monte Carlo simulations that consider extreme values of calibration uncertainty (CU). The pulling rate in all experiments was 40 pN s^{-1}

Dual-marker OFP overcomes confounding protein dimerization. In the atomic force spectroscopy experiments reported in Figs. 2, 3, polyproteins are picked up by the AFM cantilever through non-specific physisorption. Hence, experimental traces can contain different number of unfolding events (Fig. 3b). Non-specific protein pickup also leads to the occasional appearance of traces containing more unfolding events than engineered domains in the polyprotein, an effect that results from polyprotein dimerization[29]. For instance, in Fig. 3b a few traces with n (24 nm) > 8 are identified when pulling from $(C3)_8$. Comparison of Fig. 3b, d identifies a new population of events at n(24 nm) > 4 and n(16 nm) > 1 that appear only when $(C3)_8$ and $(C3\text{-}L)_4$ are measured concurrently in the same experiment, which we interpret as heterodimers between $(C3)_8$ and $(C3\text{-}L)_4$. In the context of OFP, heterodimerization hampers proper assignment of traces, since there is a non-zero probability that some heterodimers are included in the gating region of $(C3\text{-}L)_4$. As a result, a fraction of events coming from $(C3)_8$ could be mistakenly assigned to $(C3\text{-}L)_4$.

In general, the extent of protein dimerization in single-molecule AFM is dependent on the particular experimental conditions. Hence, heterodimerization poses a challenge to OFP, whose extent may vary depending on the system to study. However, we hypothesized that difficulties coming from protein dimerization could be overcome by using a second protein marker, since traces originating from dimers would be fingerprinted by the presence of both marker proteins. We chose the protein SUMO1 as a second marker because its unfolding length is different from those ones of C3 and Protein L[30]. We engineered the heteropolyprotein $(C3\text{-}SUMO1)_4$ and pulled it in the AFM (Supplementary Fig. 2). Two population of unfolding steps at 20 and 24 nm are detected, corresponding to the unfolding of SUMO1 and C3, respectively (Supplementary Fig. 3C).

Having two marker proteins enables gating criteria that are based exclusively on the presence of the marker domains, in a manner that protein dimers can be identified and excluded from the analysis (Fig. 4a, b, Supplementary Fig. 8). According to experiments in which $(C3\text{-}L)_4$ and $(C3\text{-}SUMO1)_4$ are measured separately, we used the gating criterion that n(16 nm) > 1 and n (20 nm) = 0 marks unfolding of $(C3\text{-}L)_4$, and n(20 nm) > 1 and n (16 nm) = 0 defines unfolding of $(C3\text{-}SUMO1)_4$, which only misclassifies 1 out of 136 traces. Following this gating criterion, we determined the distribution of unfolding forces of C3 in the context of $(C3\text{-}SUMO1)_4$ and compared the results with C3 unfolding in the context of $(C3\text{-}L)_4$, both in traditional and OFP experiments (Fig. 4c, d, Table 1). Although the $\langle F_u \rangle$ of C3 in $(C3\text{-}L)_4$ appears to be 12% higher in traditional experiments ($\langle F_u \rangle$ = 79.2 and 88.4 pN for the SUMO1- and L-containing heteropolyproteins, respectively), differences vanish in OFP experiments ($\langle F_u \rangle$ = 89.5 and 90.0 pN for the SUMO1- and

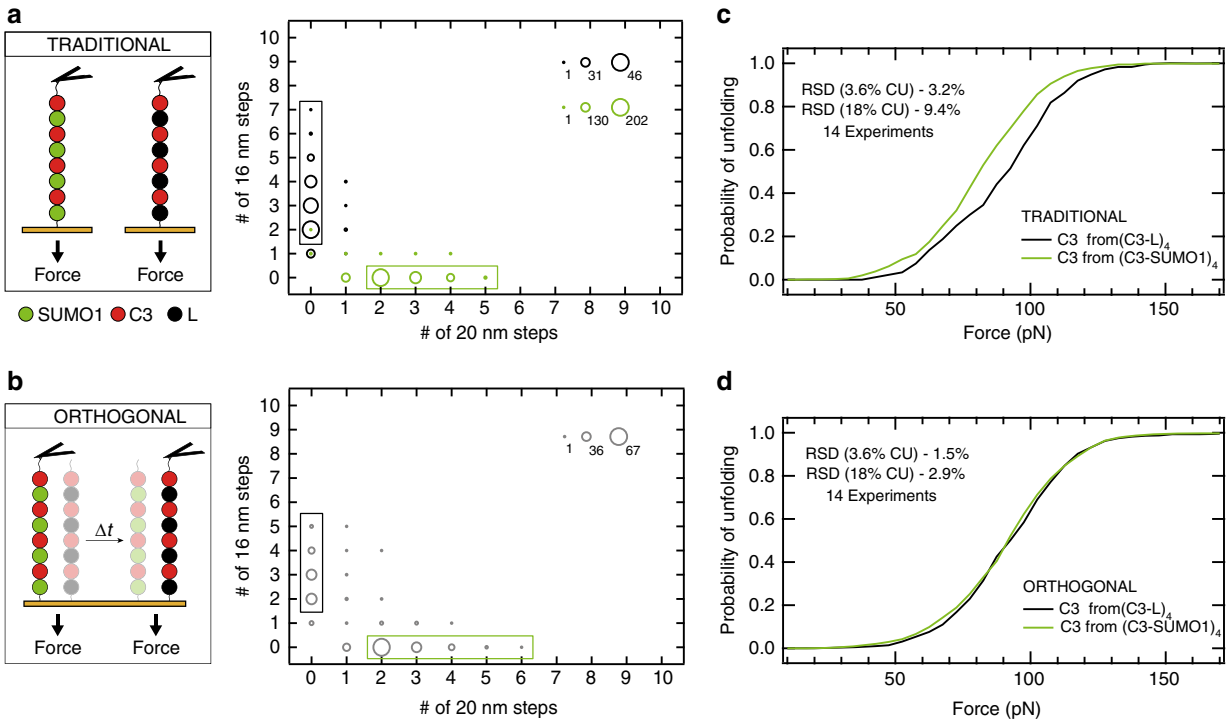

Fig. 4 Dual-marker orthogonal fingerprinting overcomes confounding protein dimerization in concurrent atomic force spectroscopy. **a** Mechanical unfolding of $(C3\text{-}SUMO1)_4$ and $(C3\text{-}L)_4$ are measured in separate traditional experiments. Individual traces are classified according to their number of 16 and 20 nm unfolding events, which mark the mechanical unfolding of Protein L and SUMO1, respectively. The plot shows the frequency of the traces that have different combination of unfolding events, as indicated by the size of the dots. Traces coming from mechanical unfolding of $(C3\text{-}SUMO1)_4$ are assigned when $n(16\,\text{nm}) = 0$ and $n(20\,\text{nm}) > 1$ (green rectangle), whereas $(C3\text{-}L)_4$ traces are identified by $n(16\,\text{nm}) > 1$ and $n(20\,\text{nm}) = 0$. Number of traces analyzed: $(C3\text{-}L)_4$, 163; $(C3\text{-}SUMO1)_4$, 525. **b** Mechanical unfolding of $(C3\text{-}SUMO1)_4$ and $(C3\text{-}L)_4$, as measured concurrently in orthogonal fingerprinting (OFP) experiments (temporal sequence is represented by Δt; the protein being pulled at each time is highlighted). The plot shows the frequency of the traces that have different combination of unfolding events, as indicated by the size of the dots (298 traces). The gating strategy defined in **a** allows the classification of the traces as originating from $(C3\text{-}SUMO1)_4$ (green rectangle) or $(C3\text{-}L)_4$ (black rectangle). **c** Experimental cumulative unfolding probability distribution of the C3 domain in the context of $(C3\text{-}L)_4$ (6 experiments, 177 events, black; data are also presented in Fig. 3c) and $(C3\text{-}SUMO1)_4$ (8 experiments, 742 events, green), as measured in traditional experiments. **d** Experimental cumulative unfolding probability distribution of the C3 domain in the context of $(C3\text{-}L)_4$ (873 events, black) and $(C3\text{-}SUMO1)_4$ (1043 events, green), resulting from unfolding data obtained in 14 independent OFP experiments. Relative standard deviation (RSD) values in the insets in **c**, **d** are estimated using Monte Carlo simulations that consider extreme values of calibration uncertainty (CU). The pulling rate in all experiments was 40 pN s^{-1}

Table 1 Mechanical characterization of C3 by single-molecule atomic force spectroscopy

AFM mode	Protein	C3, $\langle F_u \rangle$ (pN)	n_{exp}	n_{events}	RSD at 3.6% CU (%)	RSD at 18% CU (%)
Traditional	$(C3)_8$	90.7	11	1334	3.0	8.2
	$(C3\text{-}L)_4$	88.4	6	177	N/A	N/A
	$(C3\text{-}SUMO1)_4$	79.2	8	742	3.2	9.4
OFP, single marker	$(C3)_8$	96.3	5	625	2.2	4.0
	$(C3\text{-}L)_4$	93.4	5	311	N/A	N/A
OFP, dual marker	$(C3\text{-}L)_4$	90.0	14	873	N/A	N/A
	$(C3\text{-}SUMO1)_4$	89.5	14	1043	1.5	2.9

The table summarizes results regarding mechanical characterization of the C3 domain in the context of three different polyproteins, following traditional atomic force microscopy (AFM) or orthogonal fingerpriting (OFP)-based concurrent measurements. n_{exp} and n_{events} represent the number of experiments and unfolding events, respectively. Relative standard deviations (RSDs) of the distributions of $\Delta\langle F_u \rangle$ with respect to $(C3\text{-}L)_4$ at two different calibration uncertainties (CU) were estimated by Monte Carlo simulations using the actual structure of the experimental datasets. *N/A* not applicable

L-containing heteropolyproteins, respectively). The RSD of the distribution of $\Delta\langle F_u \rangle$, as estimated from Monte Carlo simulations fed with the actual number of experiments and events, is 2–3 times smaller in OFP than in the traditional strategy (Fig. 4c, d, Table 1, Supplementary Fig. 7B)

A model for error propagation in atomic force spectroscopy. Our Monte Carlo simulations show that the improvement in accuracy in $\Delta\langle F_u \rangle$ of concurrent atomic force spectroscopy is preserved when multiple AFM experiments are averaged, and is independent of calibration uncertainty (Fig. 2g, h). In apparent contradiction, we found that the RSDs of the distributions of $\Delta\langle F_u \rangle$ calculated for OFP concurrent datasets increase with calibration uncertainty (Table 1). Here, we propose a model for the propagation of calibration errors in concurrent single-molecule force spectroscopy AFM experiments that accounts for all those observations. Considering that every unfolding force measured in

the AFM is affected by an error δ as a consequence of inaccurate force calibration, the following equation for the measured $\Delta\langle F_u\rangle$ can be derived (Supplementary Note 3):

$$\Delta<F_u>^{\text{measured}} = \Delta<F_u>^{\text{real}} + \sum_{j=1}^{n_{\text{exp}}} \bar{\delta}_j \cdot \left(\frac{n_{\text{prot1},j}}{n_{\text{events,prot1}}} - \frac{n_{\text{prot2},j}}{n_{\text{events,prot2}}} \right). \quad (1)$$

In Eq. 1, $\Delta\langle F_u\rangle^{\text{real}}$ is the value of $\Delta\langle F_u\rangle$ that would be measured if there was no error in calibration, n_{exp} is the number of experiments, $n_{\text{prot1,j}}$ and $n_{\text{prot2,j}}$ are the number of unfolding events for both proteins being compared in concurrent experiment j, $n_{\text{events,prot1}}$ and $n_{\text{events,prot2}}$ are the total number of unfolding events for each protein considering all experiments, and $\bar{\delta}_j$ is the average value of the error in force in experiment j, which is considered to be equivalent for two proteins measured concurrently.

Equation 1 shows that in concurrent measurements, $\Delta\langle F_u\rangle^{\text{measured}}$ can differ from $\Delta\langle F_u\rangle^{\text{real}}$ according to the magnitude of $\bar{\delta}_j$ values, which originate from the uncertainty in calibration, and to the specific number of unfolding events obtained for each protein in the different experiments contributing to the dataset. Importantly, if the proportion of events for both proteins is constant in all experiments ("balanced" condition: $n_{\text{prot1},j} = \text{constant} \cdot n_{\text{prot2},j}$), Eq. 1 leads to $\Delta\langle F_u\rangle^{\text{measured}} = \Delta\langle F_u\rangle^{\text{real}}$, that is, the relative mechanical stability measured in concurrent experiments is not affected by errors in calibration, independently of the number of experiments contributing to the dataset. Monte Carlo simulations readily confirm this prediction. While simulations of two concurrent experiments with 100 events per protein show that the resulting RSD of the distribution of $\Delta\langle F_u\rangle$ does not depend on the uncertainty in calibration, breaking the balanced condition by considering $n_{\text{prot1,exp1}} = n_{\text{prot2,exp2}} = 150$ and $n_{\text{prot1,exp2}} = n_{\text{prot2,exp1}} = 50$, results in a dramatic increase of RSD, especially at higher calibration uncertainties (Fig. 5a). Under these unbalanced conditions, the performance of the concurrent strategy diminishes drastically and the obtained RSD approaches the one obtained in traditional atomic force spectroscopy (Fig. 5a).

Since unbalanced data distributions result in poorer performance of concurrent atomic force spectroscopy, we examined whether balancing datasets through data removal could result in improved accuracy in $\Delta\langle F_u\rangle$. We did Monte Carlo simulations of two concurrent experiments in which $n_{\text{prot1},j} = n_{\text{prot2},j} = 50$, that is, we trimmed 100 extra events per protein so that both experiments had the same number of unfolding events for both proteins. As expected, the RSD of the distribution of $\Delta\langle F_u\rangle$ after trimming becomes independent of the calibration uncertainty (Fig. 5a). Even though having less events per experiment results *per se* in poorer definition of distributions of unfolding forces (Fig. 2e, Supplementary Fig. 5B), the RSDs of the distributions of $\Delta\langle F_u\rangle$ obtained using trimmed datasets become lower than in the case of the more populated, but unbalanced, dataset at calibration uncertainties higher than 6% (Fig. 5a).

Concurrent single-molecule atomic force spectroscopy datasets are expected to be unbalanced, since the different proteins are picked up randomly by the AFM cantilever (Fig. 1, Supplementary Table 1). We have tested whether balancing our experimental OFP datasets also leads to improved accuracy in $\Delta\langle F_u\rangle$. To this end, we have removed unfolding events so that every OFP experiment verifies the balanced condition $n_{\text{prot1}} = n_{\text{prot2}}$. Using Monte Carlo simulations, we estimate that the RSD of the distribution of $\Delta\langle F_u\rangle$ obtained from the trimmed OFP datasets becomes lower than the original RSD also at calibration uncertainties higher than 6–7% (Supplementary Fig. 7). In the two OFP datasets analyzed, the differences between the balanced and the unbalanced conditions are less prominent than in the case of artificial datasets consisting of only two experiments (Fig. 5a). Indeed, we find that the extent of improvement in performance by dataset trimming decreases with the number of experiments (Supplementary Fig. 9). Hence, we recommend that improvement in performance by balancing datasets is estimated on a case-by-case basis using Monte Carlo simulations fed with actual experimental data, as we have done here.

Discussion

In this report, we address a main limitation of force spectroscopy by AFM that arises from uncertain calibration of cantilevers. We have quantified the extent to which concurrent measurements result in improvements in the determination of relative mechanical properties by atomic force spectroscopy. We propose that concurrent AFM measurements of relative mechanical properties of cells, materials, and tissues can result in gains in performance similar to those described here for proteins. Remarkably, concurrent strategies can be achieved by adapting already available atomic force spectroscopy techniques based on fluorescent labelling of cells or polymer blends[31,32].

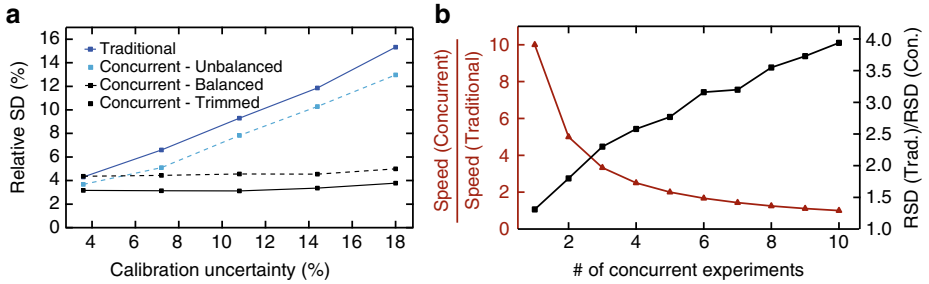

Fig. 5 Improved accuracy and throughput of concurrent atomic force spectroscopy. **a** Monte Carlo simulations show that balancing datasets obtained in concurrent experiments improves the relative standard deviation (RSD) of distributions of $\Delta\langle F_u\rangle$ at calibration uncertainties >6%. Simulations of balanced datasets (solid lines, 100 events per experiment and protein) considered two experiments per protein in traditional (blue), and two experiments in concurrent atomic force spectroscopy (black). To simulate unbalanced datasets, uneven number of unfolding events (50/150) was considered for both proteins in the first simulated experiment, and the order was reversed in the second simulated experiment (dashed blue line). The effects of balancing datasets ("trimming") were examined by running simulations at the lowest number of events for both experiments (50, dashed black line). **b** Improvement in the speed of data acquisition (red) and RSD in the distribution of $\Delta\langle F_u\rangle$ (black) by concurrent measurements are estimated using Monte Carlo simulations at 10.8% calibration uncertainty (100 events per experiment and protein). Values are compared to a situation where two proteins are measured in five traditional experiments per protein

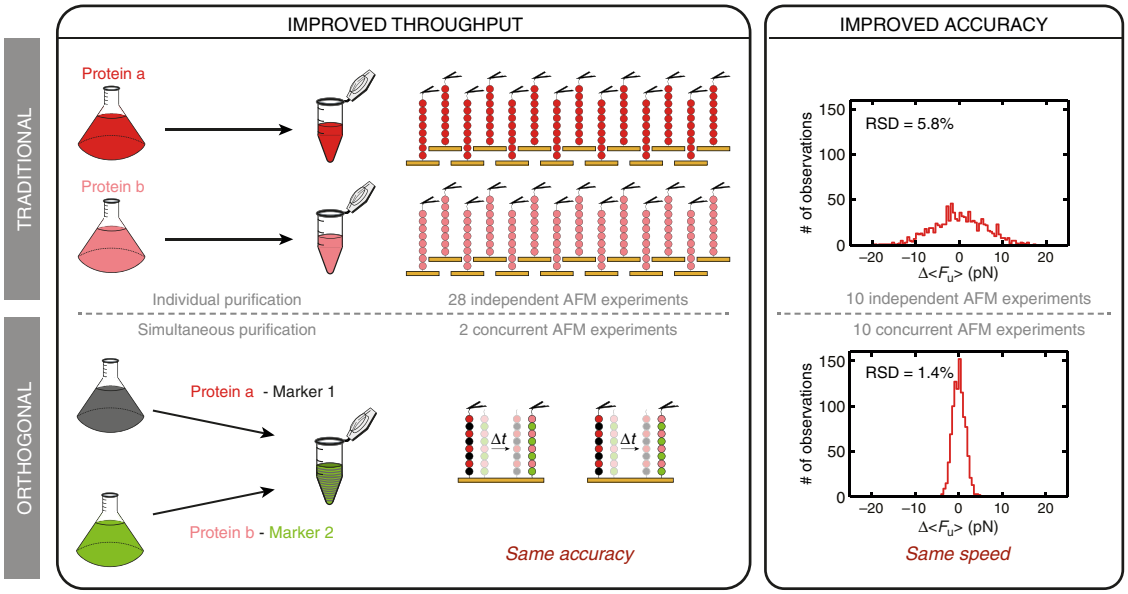

Fig. 6 Orthogonal-fingerprinting-based concurrent atomic force spectroscopy. In the traditional approach, comparison of the mechanical stability of Protein a and Protein b involves independent purification and several atomic force microscopy (AFM) experiments to compensate for inaccurate force calibration. Orthogonal fingerprinting (OFP) is based on the production of heteropolyproteins composed of the proteins of interest fused to marker domains. Since the markers provide unequivocal fingerprints in single-molecule pulling experiments, OFP enables simultaneous purification and concurrent mechanical measurements, circumventing errors in force calibration. Concurrent measurements can achieve the same accuracy in $\Delta\langle F_u\rangle$ as conventional single-molecule atomic force spectroscopy with much better throughput, as shown in the left part of the figure. Alternatively, by keeping the speed of data acquisition constant, concurrent measurements considerably improve the accuracy in the determination of $\Delta\langle F_u\rangle$, as exemplified in the right part of the figure. Improvements in throughput and accuracy are estimated from Monte Carlo simulations at 10.8% calibration uncertainty (100 events per experiment and protein)

Our work demonstrates that concurrent single-molecule atomic force spectroscopy outperforms traditional methods in several aspects (Fig. 6). First, results of concurrent atomic force spectroscopy are less affected by typical AFM experimental errors, even when multiple experiments are averaged (Fig. 2g, Supplementary Fig. 6). A major source of error in traditional force spectroscopy AFM comes from inaccurate cantilever calibration. Since the accuracy of concurrent atomic force spectroscopy is independent of calibration uncertainty, the degree of improvement is higher at high uncertainties (Fig. 2h). The uncertainty of cantilever calibration is usually considered to lie in the range of 5–25% depending on the calibration method[15], although real uncertainties are extremely challenging to estimate. We have provided an experimental lower bound of 3.6% uncertainty in cantilever calibration by the commonly used thermal fluctuations method, and showed that this uncertainty originates mainly from inaccurate determination of the deflection sensitivity (Supplementary Note 2). Uncertainties in spring constant calibration by the thermal fluctuations method have also been estimated by inter-laboratory experiments, finding a value of up to 11%[33]. Additional errors can result from the simplifications considered by calibration methods, or from difficult-to-detect defects in individual cantilevers[34]. We have considered a realistic value of 10.8% calibration uncertainty to estimate the improvements in performance by concurrent measurements described in Fig. 6. If other sources of calibration error are considered, the extent of improvement could be even better. For example, unpredictable changes in k_{sc} during experimentation due to instrument drift, material accumulation, or mechanical wear of the cantilever would, on average, affect measurements of the proteins in the sample equally. Indeed, we propose that concurrent atomic force spectroscopy strategies, in combination with available theoretical and experimental developments addressing other limitations of the AFM such as deviations from non-ideal pulling geometry[35], can be key to exploit the advantages of next-generation cantilevers, which are pushing the AFM into ranges of force, speed, stability, and time resolution at the expense of more challenging force calibration[14,36–40].

Since concurrent atomic force spectroscopy is less affected by calibration errors, the method leads to much improved accuracy in $\Delta\langle F_u\rangle$ (Figs. 2g, h, 5, 6). Keeping the speed of data acquisition constant at high calibration uncertainties, the accuracy achieved by concurrent measurements can be 6 times higher than in traditional atomic force spectroscopy (Supplementary Fig. 6B). Alternatively, concurrent atomic force spectroscopy can lead to high-throughput relative mechanical characterization of proteins (Fig. 6). We estimate that concurrent atomic force spectroscopy can obtain the data needed for the same accuracy in $\Delta\langle F_u\rangle$ over 30 times faster than traditional measurements at high calibration uncertainties (Supplementary Fig. 6C). It must be stressed that the increase in throughput and accuracy in $\Delta\langle F_u\rangle$ of concurrent atomic force spectroscopy come at the expense of each other. Although improved accuracy is the primary benefit from concurrent measurements, equivalent accuracies to traditional strategies can be reached in fewer experiments. Indeed, depending on the goals of a particular study, the experimenter can choose to favor accuracy or throughput, or to find a balance between both. For instance, in Fig. 5b, we show that different gains in accuracy and throughput can be achieved depending on the number of concurrent experiments carried out to compare unfolding forces of two proteins.

Motivated by our findings, we have developed OFP strategies for concurrent nanomechanical profiling of proteins. The increase in accuracy in $\Delta\langle F_u\rangle$ identified by Monte Carlo simulations is also captured in our limited experimental dataset, since the spread of $\Delta\langle F_u\rangle$ in pairs of OFP experiments is lower than in traditional experiments (SD = 8.0 vs. 11.2 pN, respectively) (Supplementary Fig. 10). An advantage of OFP over a previous concurrent strategy based on patterning of proteins[22,23] is that it can be readily implemented in any atomic force spectroscopy setup. In addition, different fingerprinting lengths in OFP provide

additional reassurance of the identity of the probed proteins. In this regard, OFP is very well suited to compare mechanical properties of proteins with similar unfolding lengths. Hence, OFP can define mechanical hierarchies in multidomain proteins with higher accuracy, and lead to better descriptions of the mechanical effects of mutations, post-translational modifications, and the chemical environment on proteins and their complexes[41–46]. Indeed, our highly accurate OFP experiments show that the mechanical stabilities of the C3 domain in the context of a $(C3)_8$ homopolyprotein, or within a $(C3\text{-}L)_4$ or $(C3\text{-}SUMO1)_4$, are very similar (Figs. 3e, 4d, Table 1). The fact that the mechanical stability of C3 does not depend on the neighboring marker domains lends strong support to the use of heteropolyproteins in force spectroscopy AFM[28,47–49]. Another advantage of OFP is that orthogonally fingerprinted proteins can be purified simultaneously (Supplementary Figs. 2 and 11), resulting in extra savings in working time and reagents and ensuring equal experimental conditions for both proteins (Fig. 6). Taking into account the full experimental workflow of single-molecule atomic force spectroscopy experiments, we estimate that the increase in throughput described in Fig. 6 results in ~4 times less total experimentation time (Supplementary Fig. 12). To engineer heteropolyproteins for OFP, it is important to consider the unfolding length of the protein of interest, so that marker proteins with different unfolding lengths can be chosen. If the unfolding length of the protein of interest is unknown, we recommend to build on available protein structural information to make a reasonable guess than can guide heteropolyprotein design, minimizing the probability of delays in the event that unfolding lengths match[26].

It has been proposed that the unfolding force of a reference protein can be used as an internal standard to benchmark mechanical data obtained for new proteins, a strategy that would limit the impact of calibration errors in single-molecule atomic force spectroscopy[20]. Our Monte Carlo simulations readily show that the internal standard strategy leads to much better accuracy than traditional AFM at high calibration uncertainties (Supplementary Fig. 13A). However, this strategy can lead to 100% increase in the RSD of the distribution of $\Delta\langle F_u\rangle$ as compared to concurrent methods (Supplementary Fig. 13B–E). Our simulations show that the better performance of concurrent measurements compared to the internal standard strategy is independent of the total number of events and experiments considered (Supplementary Fig. 13C). This lower performance probably stems from the fact that the internal standard strategy requires the sampling of unfolding force distributions of the reference protein, which always has an associated experimental error.

We envision two features of OFP that can be further optimized. Since the relative performance of OFP is better at high number of events per experiment (Fig. 2g, Supplementary Note 4), we propose that further improvements can be achieved by taking advantage of highly efficient high-strength single-molecule tethering methods[23,29,50]. In addition, OFP strategies hold the promise of further parallelization by the use of multiple marker proteins. Importantly, in those cases where proteins have different unfolding lengths, concurrent single-molecule AFM measurements are of immediate application, leading to the increase in accuracy and throughput described here[21]. Examples that could benefit from application of concurrent measurements include examination of the effect of disulfide bonds, protein misfolding, multimerization, and pulling geometry in the mechanical stability of proteins and their complexes[51–58], and determination of rates of force-activated chemical reactions[59]. In these examples, our Monte Carlo simulations can be applied to guide experimental design and interpretation (Supplementary Code).

Methods

Monte Carlo simulations. Monte Carlo simulations were programmed in Igor 6 (Wavemetrics). Simulations randomly assign an error in force according to a set uncertainty in the calibration between 3.6 and 18% (Supplementary Note 2). Every simulated atomic force spectroscopy experiment is therefore affected by a different calibration error, except under the condition of concurrent measurements, in which two proteins are probed in the same experiment and share error in force. Each cycle of the simulations returns a value of $\Delta\langle F_u\rangle$ for two proteins using Gaussian fits to their distribution of unfolding forces, obtained from a given number of independent experiments and unfolding events. We used a bin size of 25 pN when simulating artificial datasets, or 5 pN when feeding simulations with real datasets for better comparison with experimental distributions. Simulations calculate the RSD of the $\Delta\langle F_u\rangle$ distribution obtained from 1000 cycles of the procedure. RSD is defined as the SD of the distribution of $\Delta\langle F_u\rangle$, normalized by the theoretical value of $\langle F_u\rangle$[24].

Distributions of unfolding forces are calculated through a kinetic Monte Carlo routine that considers that protein unfolding is exponentially dependent on force according to the Bell's model[60]:

$$r = r_0 e^{F\Delta x/k_b T}. \quad (2)$$

In Eq. 2, r is the rate of protein unfolding, r_0 is the rate of unfolding at zero force, F is the force experienced by the protein, Δx is the distance to the transition state, k_b is the Boltzmann constant, and T is the absolute temperature. In the simulations, we considered that $k_b T = 4.11$ pN nm, $r_0 = 0.01\ s^{-1}$, and $\Delta x = 0.2$ nm. We chose these values because they are a good estimate of mechanical unfolding parameters of C3. We checked that values of RSD are fairly insensitive to small variations in r_0 and Δx, and therefore one single set of parameters is enough to calculate RSD of distributions of $\Delta\langle F_u\rangle$ even if the mechanical parameters of the proteins to be compared are slightly different (Supplementary Table 2).

The kinetic Monte Carlo to obtain distribution of unfolding forces compares a random number with the instantaneous probability of unfolding at a given force. If the unfolding probability is higher than the random number, unfolding is considered to happen at that force. Instantaneous probabilities of unfolding are calculated following a linear approximation[61]:

$$P_u = n r_0 e^{F\varepsilon\Delta x/k_b T}\delta t. \quad (3)$$

In Eq. 3, n is the number of domains that remain folded at a particular force, ε is the error in force due to the uncertain cantilever calibration (Supplementary Note 2), and δt is the time step of the Monte Carlo. In the simulations, we used $\delta t = 10^{-4}$ s, which ensures validity of the linear approximation, since $nr\delta t$ is kept under 0.05 (Supplementary Note 5). Pilot simulations show that results do not vary if we use a smaller time step of 10^{-5} s.

In the internal standard strategy, protein mean unfolding force values are corrected according to:

$$\langle F_u\rangle_{corr} = \langle F_u\rangle \frac{\langle F_u\rangle_{reference}}{\langle F_u\rangle_{reference}^{measured}}, \quad (4)$$

where $\langle F_u\rangle_{reference}$ is the calibrated value of the mean unfolding force for the reference protein and $\langle F_u\rangle_{reference}^{measured}$ is the actual mean unfolding force obtained by the Monte Carlo routine. We did simulations considering Protein L ($r_0 = 0.05\ s^{-1}$ and $\Delta x = 0.22$ nm)[62] or SUMO1 ($r_0 = 1.1 \times 10^{-5}\ s^{-1}$ and $\Delta x = 0.51$ nm)[30] as reference proteins.

Protein production and purification. The complementary DNAs (cDNAs) coding for the C3-L and C3-SUMO1 constructs were produced by gene synthesis (NZY-Tech and Gene Art, respectively). The cDNA coding for the C3 domain was obtained by PCR. cDNAs coding for polyproteins were produced following an iterative strategy of cloning using *Bam*HI, *Bgl*II, and *Kpn*I restriction enzymes[27,63]. Final cDNAs were inserted in the pQE80L expression plasmid using *Bam*HI and *Kpn*I and the resulting plasmids were verified by Sanger sequencing. Full protein sequences are reported in Supplementary Note 1. Polyproteins were expressed in BLR (DE3) *Escherichia coli* strain. Briefly, fresh cultures ($OD_{600} = 0.6$–1.0) are induced with 1 mM isopropyl β-D-1-thiogalactopyranoside for 3 h at 37 °C and at 250 rpm. Cells are lysed by a combination of tip sonication and passes through a French Press. Polyproteins are purified from the soluble fraction through Ni-NTA agarose chromatography (Qiagen), following the recommendations of the supplier and adding 10 mM dithiothreitol to the buffers. Further purification is achieved by size-exclusion chromatography in an AKTA Pure 25L system using a Superose 6 Increase 10/300 GL or a Superdex 200 Increase 10/300 GL column (GE Healthcare). The proteins are eluted in 10 mM HEPES, pH 7.2, 150 mM NaCl, 1 mM EDTA, which is also the buffer used in atomic force spectroscopy experiments. Purity of samples was evaluated using sodium dodecyl sulfate-polyacrylamide electrophoresis gels (a typical result is shown in Supplementary Fig. 2).

Force spectroscopy by AFM. Single-molecule AFM measurements were obtained in an AFS setup (Luigs & Neumann) according to established protocols[7]. Polyproteins include two C-terminal cysteine residues for covalent attachment to gold-coated coverslips (Luigs & Neumann). We used silicon nitride MLCT-C cantilevers

with a 60-nm gold back side coating (Bruker), which we calibrated according to the thermal fluctuations method[64]. Typical spring constant values ranged between 15 and 20 pN nm^{-1}. To run single-molecule AFM experiments, a small aliquot (2–10 μL) of the purified protein is deposited on the gold-coated coverslip, or directly into the HEPES buffer contained in the fluid chamber of the AFS. The cantilever is brought in contact to the surface for 1–2 s at 500–2000 pN to favor formation of single-molecule tethers by non-specific physisorption, resulting in protein tethers containing variable number of domains[7,29]. Then, the surface is retracted to achieve the set point force. If a single-molecule tether is formed, the force is increased linearly at 40 pN s^{-1} for 5 s while the length of the polyprotein is measured. This protocol ensures full unfolding of C3, L, and SUMO1 domains (Supplementary Fig. 3). Unfolding events are detected as increases in the length of the protein. In the initial characterization of polyproteins, we analyzed all traces that contain at least two events of the same size, which allows to set a fingerprinting length for the domains (24 ± 1 nm for C3, 16 ± 1 nm for protein L, and 20 ± 1 nm for SUMO1, see Supplementary Fig. 3). For the estimation of experimental F_u, we only considered traces that contain fingerprinting unfolding lengths according to stringent gating criteria validated in traditional, separate AFM experiments (Figs. 3b, d, 4a, b)[7]. Unfolding forces were recorded and plotted as cumulative distributions. $\langle F_u \rangle$ values were obtained directly from Gaussian fits to the experimental histograms of unfolding forces. Force inaccuracy due to laser interference was lower than 40 pN in all experiments (peak-to-peak height in baseline force-extension recordings)[7].

Data availability

Data is available on reasonable request to the corresponding author.

Code availability

The code for the Monte Carlo simulations is available online as Supplementary Code.

Received: 14 November 2018 Accepted: 5 July 2019
Published online: 02 August 2019

References

1. Binnig, G., Quate, C. F. & Gerber, C. Atomic force microscope. *Phys. Rev. Lett.* **56**, 930–933 (1986).
2. Garcia, R. & Herruzo, E. T. The emergence of multifrequency force microscopy. *Nat. Nanotechnol.* **7**, 217–226 (2012).
3. Krieg, M. et al. Atomic force microscopy-based mechanobiology. *Nat. Rev. Phys.* **1**, 41–57 (2018).
4. Ando, T., Uchihashi, T. & Kodera, N. High-speed AFM and applications to biomolecular systems. *Annu. Rev. Biophys.* **42**, 393–414 (2013).
5. Al-Rekabi, Z. & Contera, S. Multifrequency AFM reveals lipid membrane mechanical properties and the effect of cholesterol in modulating viscoelasticity. *Proc. Natl. Acad. Sci. USA* **115**, 2658–2663 (2018).
6. Lai, C.-Y., Santos, S. & Chiesa, M. Systematic multidimensional quantification of nanoscale systems from bimodal atomic force microscopy data. *ACS Nano* **10**, 6265–6272 (2016).
7. Popa, I., Kosuri, P., Alegre-Cebollada, J., Garcia-Manyes, S. & Fernandez, J. M. Force dependency of biochemical reactions measured by single-molecule force-clamp spectroscopy. *Nat. Protoc.* **8**, 1261–1276 (2013).
8. Neuman, K. C. & Nagy, A. Single-molecule force spectroscopy: optical tweezers, magnetic tweezers and atomic force microscopy. *Nat. Methods* **5**, 491–505 (2008).
9. Rief, M., Gautel, M., Oesterhelt, F., Fernandez, J. M. & Gaub, H. E. Reversible unfolding of individual titin immunoglobulin domains by AFM. *Science* **276**, 1109–1112 (1997).
10. Linke, W. A. & Hamdani, N. Gigantic business: titin properties and function through thick and thin. *Circ. Res.* **114**, 1052–1068 (2014).
11. del Rio, A. et al. Stretching single talin rod molecules activates vinculin binding. *Science* **323**, 638–641 (2009).
12. Paluch, E. K. et al. Mechanotransduction: use the force(s). *BMC Biol.* **13**, 47 (2015).
13. Li, H. et al. Reverse engineering of the giant muscle protein titin. *Nature* **418**, 998–1002 (2002).
14. Slattery, A. D., Blanch, A. J., Ejov, V., Quinton, J. S. & Gibson, C. T. Spring constant calibration techniques for next-generation fast-scanning atomic force microscope cantilevers. *Nanotechnology* **25**, 335705 (2014).
15. Charles, A. C. & Martin, P. S. The determination of atomic force microscope cantilever spring constants via dimensional methods for nanomechanical analysis. *Nanotechnology* **16**, 1666 (2005).
16. Killgore, J. P., Geiss, R. H. & Hurley, D. C. Continuous measurement of atomic force microscope tip wear by contact resonance force microscopy. *Small* **7**, 1018–1022 (2011).
17. Wagner, R., Moon, R., Pratt, J., Shaw, G. & Raman, A. Uncertainty quantification in nanomechanical measurements using the atomic force microscope. *Nanotechnology* **22**, 455703 (2011).
18. Schillers, H. et al. Standardized nanomechanical atomic force microscopy procedure (SNAP) for measuring soft and biological samples. *Sci. Rep.* **7**, 5117 (2017).
19. Anderson, B. R., Bogomolovas, J., Labeit, S. & Granzier, H. Single molecule force spectroscopy on titin implicates immunoglobulin domain stability as a cardiac disease mechanism. *J. Biol. Chem.* **288**, 5303–5315 (2013).
20. Sadler, D. P. et al. Identification of a mechanical rheostat in the hydrophobic core of protein L. *J. Mol. Biol.* **393**, 237–248 (2009).
21. Jobst, M. A. et al. Resolving dual binding conformations of cellulosome cohesin-dockerin complexes using single-molecule force spectroscopy. *eLife* **4**, e10319 (2015).
22. Otten, M. et al. From genes to protein mechanics on a chip. *Nat. Methods* **11**, 1127–1130 (2014).
23. Verdorfer, T. et al. Combining in vitro and in silico single-molecule force spectroscopy to characterize and tune cellulosomal scaffoldin mechanics. *J. Am. Chem. Soc.* **139**, 17841–17852 (2017).
24. Schlierf, M., Li, H. & Fernandez, J. M. The unfolding kinetics of ubiquitin captured with single-molecule force-clamp techniques. *Proc. Natl. Acad. Sci. USA* **101**, 7299–7304 (2004).
25. Alegre-Cebollada, J. et al. S-glutathionylation of cryptic cysteines enhances titin elasticity by blocking protein folding. *Cell* **156**, 1235–1246 (2014).
26. Carrion-Vazquez, M. et al. Mechanical design of proteins studied by single-molecule force spectroscopy and protein engineering. *Prog. Biophys. Mol. Biol.* **74**, 63–91 (2000).
27. Carrion-Vazquez, M. et al. Mechanical and chemical unfolding of a single protein: a comparison. *Proc. Natl. Acad. Sci. USA* **96**, 3694–3699 (1999).
28. Li, H. et al. Multiple conformations of PEVK proteins detected by single-molecule techniques. *Proc. Natl. Acad. Sci. USA* **98**, 10682–10686 (2001).
29. Popa, I. et al. Nanomechanics of HaloTag tethers. *J. Am. Chem. Soc.* **135**, 12762–12771 (2013).
30. Kotamarthi, H. C., Sharma, R. & Koti Ainavarapu, S. R. Single-molecule studies on PolySUMO proteins reveal their mechanical flexibility. *Biophys. J.* **104**, 2273–2281 (2013).
31. Herruzo, E. T., Perrino, A. P. & Garcia, R. Fast nanomechanical spectroscopy of soft matter. *Nat. Commun.* **5**, 3126 (2014).
32. Bhat, S. V. et al. Correlative atomic force microscopy quantitative imaging-laser scanning confocal microscopy quantifies the impact of stressors on live cells in real-time. *Sci. Rep.* **8**, 8305 (2018).
33. te Riet, J. et al. Interlaboratory round robin on cantilever calibration for AFM force spectroscopy. *Ultramicroscopy* **111**, 1659–1669 (2011).
34. Ohler, B. *Practical Advice on the Determination of Cantilever Spring Constants*. Technical Report (Veeco Instruments Incorporated, Santa Barbara, 2007).
35. Walder, R., Van Patten, W. J., Adhikari, A. & Perkins, T. T. Going vertical to improve the accuracy of atomic force microscopy based single-molecule force spectroscopy. *ACS Nano* **12**, 198–207 (2018).
36. Rico, F., Gonzalez, L., Casuso, I., Puig-Vidal, M. & Scheuring, S. High-speed force spectroscopy unfolds titin at the velocity of molecular dynamics simulations. *Science* **342**, 741–743 (2013).
37. Yu, H., Siewny, M. G., Edwards, D. T., Sanders, A. W. & Perkins, T. T. Hidden dynamics in the unfolding of individual bacteriorhodopsin proteins. *Science* **355**, 945–950 (2017).
38. He, C. et al. Direct observation of the reversible two-state unfolding and refolding of an alpha/beta protein by single-molecule atomic force microscopy. *Angew. Chem.* **54**, 9921–9925 (2015).
39. Faulk, J. K., Edwards, D. T., Bull, M. S. & Perkins, T. T. Improved force spectroscopy using focused-ion-beam-modified cantilevers. *Methods Enzymol.* **582**, 321–351 (2017).
40. Uhlig, M. R., Amo, C. A. & Garcia, R. Dynamics of breaking intermolecular bonds in high-speed force spectroscopy. *Nanoscale* **10**, 17112–17116 (2018).
41. Oroz, J. et al. The Y9P variant of the titin I27 module: structural determinants of its revisited nanomechanics. *Structure* **24**, 606–616 (2016).
42. Li, H., Carrion-Vazquez, M., Oberhauser, A. F., Marszalek, P. E. & Fernandez, J. M. Point mutations alter the mechanical stability of immunoglobulin modules. *Nat. Struct. Biol.* **7**, 1117–1120 (2000).
43. Oberhauser, A. F., Badilla-Fernandez, C., Carrion-Vazquez, M. & Fernandez, J. M. The mechanical hierarchies of fibronectin observed with single-molecule AFM. *J. Mol. Biol.* **319**, 433–447 (2002).
44. Li, H., Oberhauser, A. F., Fowler, S. B., Clarke, J. & Fernandez, J. M. Atomic force microscopy reveals the mechanical design of a modular protein. *Proc. Natl. Acad. Sci. USA* **97**, 6527–6531 (2000).
45. Williams, P. M. et al. Hidden complexity in the mechanical properties of titin. *Nature* **422**, 446–449 (2003).

46. Milles, L. F., Schulten, K., Gaub, H. E. & Bernardi, R. C. Molecular mechanism of extreme mechanostability in a pathogen adhesin. *Science* **359**, 1527–1533 (2018).
47. Dietz, H. & Rief, M. Exploring the energy landscape of GFP by single-molecule mechanical experiments. *Proc. Natl. Acad. Sci. USA* **101**, 16192–16197 (2004).
48. Steward, A., Toca-Herrera, J. L. & Clarke, J. Versatile cloning system for construction of multimeric proteins for use in atomic force microscopy. *Protein Sci.* **11**, 2179–2183 (2002).
49. Oroz, J., Hervás, R. & Carrión-Vázquez, M. Unequivocal single-molecule force spectroscopy of proteins by AFM using pFS vectors. *Biophys. J.* **102**, 682–690 (2012).
50. Zakeri, B. et al. Peptide tag forming a rapid covalent bond to a protein, through engineering a bacterial adhesin. *Proc. Natl. Acad. Sci. USA* **109**, E690–E697 (2012).
51. Giganti, D., Yan, K., Badilla, C. L., Fernandez, J. M. & Alegre-Cebollada, J. Disulfide isomerization reactions in titin immunoglobulin domains enable a mode of protein elasticity. *Nat. Commun.* **9**, 185 (2018).
52. Manteca, A. et al. Mechanochemical evolution of the giant muscle protein titin as inferred from resurrected proteins. *Nat. Struct. Mol. Biol.* **24**, 652–657 (2017).
53. Manteca, A. et al. The influence of disulfide bonds on the mechanical stability of proteins is context dependent. *J. Biol. Chem.* **292**, 13374–13380 (2017).
54. Bertz, M., Buchner, J. & Rief, M. Mechanical stability of the antibody domain CH3 homodimer in different oxidation states. *J. Am. Chem. Soc.* **135**, 15085–15091 (2013).
55. Carrion-Vazquez, M. et al. The mechanical stability of ubiquitin is linkage dependent. *Nat. Struct. Biol.* **10**, 738–743 (2003).
56. Oberhauser, A. F., Marszalek, P. E., Carrion-Vazquez, M. & Fernandez, J. M. Single protein misfolding events captured by atomic force microscopy. *Nat. Struct. Biol.* **6**, 1025–1028 (1999).
57. Sarkar, A., Caamano, S. & Fernandez, J. M. The mechanical fingerprint of a parallel polyprotein dimer. *Biophys. J.* **92**, L36–L38 (2007).
58. Carl, P., Kwok, C. H., Manderson, G., Speicher, D. W. & Discher, D. E. Forced unfolding modulated by disulfide bonds in the Ig domains of a cell adhesion molecule. *Proc. Natl. Acad. Sci. USA* **98**, 1565–1570 (2001).
59. Garcia-Manyes, S., Liang, J., Szoszkiewicz, R., Kuo, T. L. & Fernandez, J. M. Force-activated reactivity switch in a bimolecular chemical reaction. *Nat. Chem.* **1**, 236–242 (2009).
60. Bell, G. I. Models for the specific adhesion of cells to cells. *Science* **200**, 618–627 (1978).
61. Shi, J., Gafni, A. & Steel, D. Simulated data sets for single molecule kinetics: some limitations and complications of data analysis. *Eur. Biophys. J.* **35**, 633–645 (2006).
62. Brockwell, D. J. et al. Mechanically unfolding the small, topologically simple protein L. *Biophys. J.* **89**, 506–519 (2005).
63. Alegre-Cebollada, J., Badilla, C. L. & Fernandez, J. M. Isopeptide bonds block the mechanical extension of pili in pathogenic Streptococcus pyogenes. *J. Biol. Chem.* **285**, 11235–11242 (2010).
64. Hutter, J. L. & Bechhoefer, J. Calibration of atomic-force microscope tips. *Rev. Sci. Instrum.* **64**, 1868–1873 (1993).

Acknowledgements

J.A.-C. acknowledges funding from the Ministerio de Ciencia, Innovación y Universidades (MCNU) through grants BIO2014-54768-P, BIO2017-83640-P (AEI/FEDER, UE), and RYC-2014-16604, the European Research Area Network on Cardiovascular Diseases (ERA-CVD/ISCIII, MINOTAUR, AC16/00045), the *Comunidad de Madrid* (P2018/NMT-4443), and the CNIC-Severo Ochoa intramural grant program (03-2016 IGP). The CNIC is supported by the Instituto de Salud Carlos III (ISCIII), MCNU and the Pro CNIC Foundation, and is a Severo Ochoa Center of Excellence (SEV-2015-0505). C.P.-L. was a recipient of CNIC Master Fellowship. C.S.-C. is the recipient of an FPI predoctoral fellowship BES-2016-076638. We thank Natalia Vicente for excellent technical support (through grant PEJ16/MED/TL-1593 from *Comunidad de Madrid*). We thank all the members of the laboratory of Molecular Mechanics of the Cardiovascular System for helpful discussions. We also thank Elías Herrero-Galán (CNIC, Madrid) for critical reading of the manuscript, Lidia Prieto-Frías for key insights about propagation of calibration errors, and the reviewers of the manuscript for constructive comments.

Author contributions

J.A.-C. designed the research. D.V.-C engineered polyprotein constructs and produced proteins. C.P.-L., C.S.-C. and D.S.-O. did AFM experiments and analyzed single-molecule data. J.A.-C. programmed Monte Carlo simulations. C.P.-L., C.S.-C. and J.A.-C. run and analyzed Monte Carlo simulations and assembled display figures. J.A.-C. drafted the manuscript with input from all the authors.

Additional information

Supplementary information accompanies this paper at https://doi.org/10.1038/s42005-019-0192-y.

Competing interests: The authors declare no competing interests.

Reprints and permission information is available online at http://npg.nature.com/reprintsandpermissions/

Publisher's note: Springer Nature remains neutral with regard to jurisdictional claims in published maps and institutional affiliations.